Environmental Health Engineering and Management Journal. 2025;12:1400
http://ehemj.com
doi 10.34172/EHEM.1400

Environmental Health Engineering and Management Journal

Original Article

Environmental Health Engineering and Management

Open Access Publish Free

Comparison of the toxicity of hematite and magnetite iron oxide nanoparticles on human lung A549 cell lines

Athena Rafieepour[1], Mansour Rezazadeh Azari[2*], Rasul Nasiri[3], Jalal Pourahmad[4]

[1]Air Pollution Research Center, Department of Occupational Health Engineering and Safety, School of Public Health, Iran University of Medical Sciences, Tehran, Iran
[2]Department of Occupational Health and Safety Engineering, School of Public Health and Safety, Shahid Beheshti University of Medical Sciences, Tehran, Iran
[3]Air Pollution Research Center, Iran University of Medical Sciences, Tehran, Iran
[4]Department of Toxicology, School of Pharmacy, Shahid Beheshti University of Medical Sciences, Tehran, Iran

Abstract

Background: Today, iron oxide nanoparticles are produced in various structural shapes and formulas for industrial and medical applications. The widespread use of these nanoparticles highlights the need to consider their health effects.

Methods: A549 human lung cell lines were cultured in 24- and 72-hours time exposure with hematite nano-cylinder (ferric oxide) and magnetite nano-sphere (Ferrosoferric Oxide) in a size of < 40 nm. The toxicity of iron oxide nanoparticles at concentrations of 10, 50, 100, and 250 µg/ml on A549 cells was examined by measuring SDH activity, ROS generation, GSH content, MMP, and apoptosis-necrosis incidence rates.

Results: Hematite nanoparticles induced a significantly higher reduction in SDH activity compared to magnetite ($P < 0.05$) at concentrations of ≥ 50 µg/ml. ROS generation was higher in cells exposed to magnetite for 24 hours ($P < 0.05$) but reversed at 72 hours, where hematite induced more ROS ($P < 0.05$). MMP and intracellular GSH content were significantly lower in hematite-exposed cells than magnetite, particularly at 250 µg/ml ($P < 0.05$). Apoptosis-necrosis rates were substantially higher in hematite-exposed cells, with a 22% increase at 250 µg/ml compared to magnetite ($P < 0.05$).

Conclusion: The results show that hematite nanoparticles are more toxic than magnetite nanoparticles on A549 cells. These findings clarify the importance of choosing the type of nanoparticle and its concentration in industrial and medical applications. For future research, there is a need to investigate the toxicity mechanisms and environmental effects of these nanoparticles.

Keywords: Toxicity, Ferric oxide, Ferrosoferric oxide, Nanoparticles, A549 cells

Citation: Rafieepour A, Rezazadeh Azari M, Nasiri R, Pourahmad J. Comparison of the toxicity of hematite and magnetite iron oxide nanoparticles on human lung A549 cell lines. Environmental Health Engineering and Management Journal. 2025;12:1400. doi: 10.34172/EHEM.1400.

Article History:
Received: 29 July 2024
Revised: 13 January 2025
Accepted: 13 January 2025
ePublished: 5 August 2025

***Correspondence to:**
Mansour Rezazadeh Azari,
Email: mrazari@sbmu.ac.ir

Introduction

Currently, the development and industrialization of societies have led to the introduction of various pollutants into the environment, resulting in soil, water, and air pollution, as well as climate change (1,2). Toxic pollutants easily enter the human body through the air, leading to adverse effects on human health (3).

Iron oxides are the most frequent compounds in nature with different structural formulas: wüstite in divalent capacity (Fe^{+2}), magnetite with di- and trivalent capacity (Fe^{+2}, Fe^{+3}), hematite and magnetite with trivalent capacity (Fe^{+3}). Hematite and magnetite are the most common types of iron oxides (4,5) that have been widely used in industrial, medical, and research processes at the nanometer scale (6,7).

Today, nanotechnology is a key technology of the 21st century due to its applications in various sciences (8,9). The distinct properties of nanomaterials compared to their larger counterparts have led to their increasing application in various processes and the emergence of this new field (10). Nanotechnology is considered a revolution in future sciences (11), and its production and consumption have experienced a significant growth trend in recent years (12). Among the producing nanoparticles, iron oxide nanoparticles are the top ten nanoparticles and have a significant increase in the nanoparticles market (13,14). Magnetic nanoparticles, due to their unique properties, are widely used in medical and industrial applications (11,15). In some studies, the use of nanoparticles is presented as a double-edged sword (16). Nanoparticles have a higher surface-to-mass ratio than larger particles, which increases their biological reactivity (17-20) and can

© 2025 The Author(s). Published by Kerman University of Medical Sciences. This is an open-access article distributed under the terms of the Creative Commons Attribution License (http://creativecommons.org/licenses/by/4.0), which permits unrestricted use, distribution, and reproduction in any medium, provided the original work is properly cited.

damage the body's biological systems (17,21).

Many authors have raised concerns about human health due to the release of nanoparticles into the air, which remain suspended for a long time and could lead to pulmonary exposure (22). The release of iron oxide nanoparticles into the air is reported during the production, storage, use of the nano-product, or as a result of exposure to natural, occupational, or traffic-related processes (23,24). The primary route of exposure to environmental pollutants is through the respiratory system. The A549 cell line has been considered the most suitable human pulmonary cell line for investigating the toxicity of nanoparticles in in vitro toxicology studies (23).

According to a study, the physicochemical parameters that affect the surface reactivity and biological effects of nanoparticles include shape, size, concentration, crystalline structure, surface coating, and chemical composition (25). In some studies, the effects of particle size, concentration, and surface coating of nanoparticles on their toxicity have been investigated (10,24). Also, the oxidation state of chemical compounds affects the rate of ROS generation in cells (26). The ions in the structure of hematite iron oxide nanoparticles are in the form of trivalent Fe^{+3} cations, and magnetite nanoparticles are in the form of divalent and trivalent cations (Fe^{+2} and Fe^{+3}). Fe^{+3} ions have a greater tendency to participate in Fenton reactions and produce reactive oxygen species. Fe^{+3} ions have greater potency compared to Fe^{+2} in causing biological damage (27).

However, the scientific literature lacks comprehensive studies on how the nanoparticle's shape and chemical composition influence their toxicity. Few studies have briefly reported these effects (23,28). In a systematic review study, the shape of nanoparticles has been reported as a factor affecting their cell uptake rate. Silver nanowires have a greater penetration into the A549 cell line than their spherical shape (28). Based on these insights, we hypothesize that (1) the chemical composition of iron oxide nanoparticles influences their cytotoxicity; hematite displays greater toxic effects than magnetite (2). The shape of nanoparticles affects their cellular uptake and toxicity in A549 cell lines. Hence, this study aimed to compare the cytotoxicity of two types of iron oxide nanoparticles (hematite and magnetite with sizes less than 40 nm) on the A549 cell line.

Materials and Methods

Iron oxide nanoparticles in the size of < 40 nm and in two oxidation states of hematite (α-Fe_2O_3, CAS No. 1309-37-1) and magnetite (Fe3O4, CAS No. 1317-61-9) were purchased from US Research Nanomaterials, Inc. The purity of hematite nanoparticles (Ca: 0.024, Cr: 0.037, Mn: 0.095, P: 0.016, SiO_2: 0.134, and S: 0.120 (%)) and magnetite nanoparticles (Ca: 0.023, Cr: 0.0016, Mn: 0.086, K: 0.001, and SiO_2: 0.142 (%)) reported by the manufacturer was equal to 98%. Concentrations of 10, 50, 100, and 250 μg/ml were prepared by adding iron oxide nanoparticles to the serum-free culture medium (Dulbecco's Modified Eagles Medium, DMEM) according to previous literature (29) which, based on the studies in the field of acute toxicology, these concentrations fall within the appropriate range for assessing cellular toxicity (30). The suspension was homogenized by sonication before use.

The shape and size of iron oxide nanoparticles in both powder and suspension states in serum-free DMEM were measured by Transmission Electron Microscope (Philips CM30 - Netherlands) and Dynamic Light Scattering (DLS, Nanophox 90-246V), respectively. Germany). The electric charge of iron oxide nanoparticles was also measured using Zetasizer (Malvern, UK) at a concentration of 50 μg/ml in serum-free culture medium. Based on scientific literature (31), a negative electric charge indicates the instability of the agglomeration process, resulting in proper particle distribution in the suspension medium.

Cell culture and exposure to hematite and magnetite nanoparticles

Human lung epithelial cell line (A549) was purchased from Pasteur Institute Cell Bank (Tehran, Iran) and cultured in DMEM (GIBCO, USA) containing 10% fetal bovine serum (GIBCO, USA) and 1% penicillin-streptomycin (GIBCO, USA). The cells were maintained in an incubator at 37°C with 5% CO_2. Cells were routinely passaged once they reached 95% confluency to prevent overcrowding and to ensure their health and viability. This practice helped maintain cells in the optimal growth phase and minimized potential effects from over-confluence.

To ensure the absence of contamination, the cultured cells were routinely monitored under a phase-contrast microscope (Olympus-lX71). Any signs of contamination, such as abnormal cell morphology or the presence of unwanted microorganisms, were carefully examined. Only cultures free from visible contamination were used in experiments. The cells were considered suitable for experimentation once they reached 80% confluency. At this stage, cultured A549 cells were exposed to hematite and magnetite iron oxide nanoparticles for 24 and 72 hours. The rate of toxicity was assessed by evaluating succinate-coenzyme Q activity (succinate dehydrogenase, SDH) using the MTT assay, measuring the generation of reactive oxygen species (ROS), and determining intracellular glutathione content, mitochondrial membrane potential changes, and apoptosis-necrosis rates.

Considering the typical cell culture half-life of the A549 cell line (approximately 22 ± 2 hours), the exposure durations of 24 and 72 hours were selected, as they fall within the mid-phase of the cell proliferation cycle. Non-exposed cells were used as the control group, and toxicity rates in exposed groups were compared with those of the control. The control group cells were exposed to the

same conditions as the exposed cells, meaning they were cultured in a serum-free medium without nanoparticles. The morphology of A549 cells was examined before and after exposure to iron oxide nanoparticles using an inverted microscope (Olympus-lX71).

SDH activity test

Approximately 10,000 cells were seeded in each well of a 96-well plate and exposed to various concentrations of hematite and magnetite iron oxide nanoparticles for 24 and 72 hours. The succinate dehydrogenase (SDH) activity was then assessed using (3-(4,5-dimethylthiazol-2-yl)-2,5-diphenyl-tetrazolium bromide) (MTT, Sigma) and an ELISA plate reader (Biotek ELx800, USA) at 570 nm (32). The results were expressed as a percentage of SDH activity relative to the untreated control group.

ROS test

The rate of ROS generation was measured by exposing 10,000 cells per well in a 96-well black plate with different concentrations of iron oxide nanoparticles. Fluorescence light intensity due to the addition of reagent (DCFH-DA; Sigma Aldrich, Germany) after 24 and 72 hours of exposure time with nanoparticles was measured at an excitation wavelength of 485 nm and an emission wavelength of 525 nm by Multi-Mode Reader (Synergy)-HTX, BioTek, USA) (13). The results were expressed as a percentage in comparison to the control group. However, it is necessary to mention that DCFH-DA is particularly sensitive to hydrogen peroxide (H_2O_2), which may limit the interpretation of the results, as it does not provide a complete profile of other ROS species. However, despite these limitations, it remains a widely used method for measuring ROS in this study, as demonstrated in previous research.

GSH test

The intracellular GSH content of the A549 cell line was determined at 24 and 72 h exposure to A-iron oxide nanoparticles based on Ellman's method (44). In this test, the contents of lysed cells were exposed to 5,5′-Dithiobis [2-nitrobenzoic acid] reagent (DTNB) at a concentration of 2 mg/ml, and the yellow color obtained from the reduction of DTNB to TNB was read by an ELISA reader (Biotek ELx 800, USA) at 405 nm wavelength (33).

MMP test

Approximately 10,000 cells in each well of 96 black-plate were exposed to different concentrations of iron oxide nanoparticles for 24 and 72 hours. In this test, a culture medium containing Rhodamine 123 dye at a concentration of 2 µM was used. The penetration rate of nanoparticles into mitochondria was measured by measuring the intensity of fluorescence radiation due to the addition of Rhodamine 123 reagent by Multi-Mode Reader (Synergy-HTX, BioTek, USA) at excitation and emission wavelengths of 485 and 528 nm, respectively (34).

Apoptosis-necrosis test

1000,000 cells per 6-well plate were exposed to hematite and magnetite nanoparticles. After exposure times of 24 and 72 hours, cells were harvested and stained with Annexin-V and Propidium Iodide (PI) using eBioscience (USA) reagents. The rate of apoptosis and necrosis was then determined using flow cytometry (BD FACSCalibur, San Jose, California, USA) (35). Apoptotic cells were identified as Annexin-V positive and PI negative, while necrotic cells were identified as both Annexin-V and PI positive. The percentages of apoptotic and necrotic cells were plotted in the figure as separate groups, with apoptotic cells shown in gray and necrotic cells in black.

Statistical tests

The results of toxicity tests were analyzed using SPSS software version 21. An independent sample t-test was used to evaluate the effect of exposure time on cytotoxicity and to compare the toxicity of hematite nanoparticles with magnetite nanoparticles. Additionally, a one-way ANOVA test was used to investigate the effects of iron oxide nanoparticles on the incidence of toxicity compared to the control group. Following the ANOVA, a Tukey's post-hoc test was applied for multiple comparisons. The results of toxicity tests were considered at a significance level of 5% and presented as mean ± standard deviation (SD).

Quality control and quality assurance

To ensure the reliability and consistency of the experimental procedures, quality control (QC) and quality assurance (QA) measures were implemented throughout the study. All reagents, including nanoparticles, were procured from certified suppliers, and their properties, such as size, purity, and composition, were verified using characterization techniques like TEM and DLS before conducting the experiments.

Results

Physicochemical properties of hematite and magnetite nanoparticles

The dimensions of magnetite and hematite nanoparticles in powder states are shown in Figure 1. And their physicochemical properties suspended in DMEM are recorded in Table 1. The TEM images of magnetite and hematite nanoparticles were spherical and cylindrical, respectively.

Cell morphology

The morphology of 10^6 cells of the A549 cell line was examined before and after 24-hour exposure to a concentration of 50 µg/ml of hematite and magnetite nanoparticles, and the results showed a reduction in cell

population and shrinkage of cell size compared to the control group (Figure 2).

SDH activity rate

As shown in Figure 3, the SDH activity of the A549 cell lines exposed to hematite and magnetite nanoparticles decreased, and this phenomenon was concentration and time-dependent. The SDH activity of the A549 cell lines was lower than the control group at hematite nanoparticle concentrations higher than 10 µg/ml and magnetite nanoparticle concentrations higher than 50 µg/ml. However, in A549 cell lines exposed to magnetite nanoparticles with a concentration of 250 µg/ml for 24 hours, there was no significant difference between the control and exposed cells ($P=0.093$).

The results showed that the activity of SDH of A549 cells exposed to all concentrations (except 50 µg/ml) of hematite nanoparticles for 24 hours was higher than the cells exposed to magnetite nanoparticles ($P<0.05$). The activity of SDH in 72-hour exposure of A549 cells at all concentrations of hematite nanoparticles was higher than magnetite nanoparticles, but this difference was not statistically significant at a concentration of 10 µg/ml ($P=0.10$).

ROS generation test

The rate of ROS generation during 24 and 72 hours of exposure of the A549 cell line with hematite and magnetite nanoparticles was higher than that of the control group and showed a concentration and time-dependent increase ($P<0.05$).

As shown in Figure 4, the rate of ROS generation during 24-hour exposure with all concentrations of magnetite nanoparticles was higher than the exposure with hematite nanoparticles ($P<0.05$). However, the results were reversed during the 72-hour exposure time. This difference was not

Table 1. Physicochemical properties of hematite and magnetite nanoparticles

	Average size in powdery state (nm)	Average size in suspension state (nm)	Zeta potential (mV)
Fe_2O_3 nano-particles	20-40	96	-33±6
Fe_3O_4 nano-particles	20-40	60	-31±10

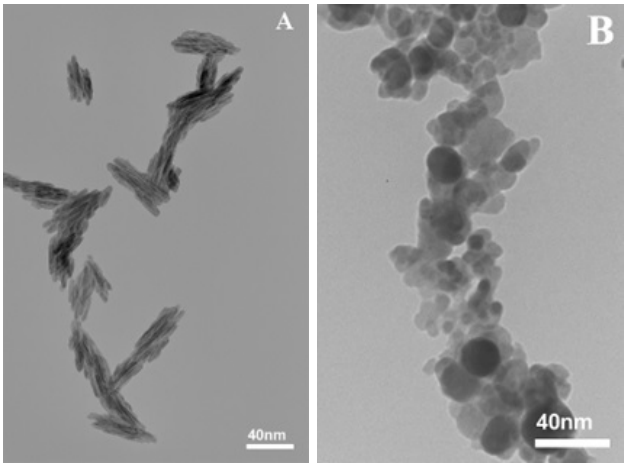

Figure 1. A: Fe_2O_3 nanoparticles (cylindrical shape) and B: Fe_3O_4 nanoparticles (spherical shape) by Transmission Electron Microscope (Philips CM30, Netherlands)

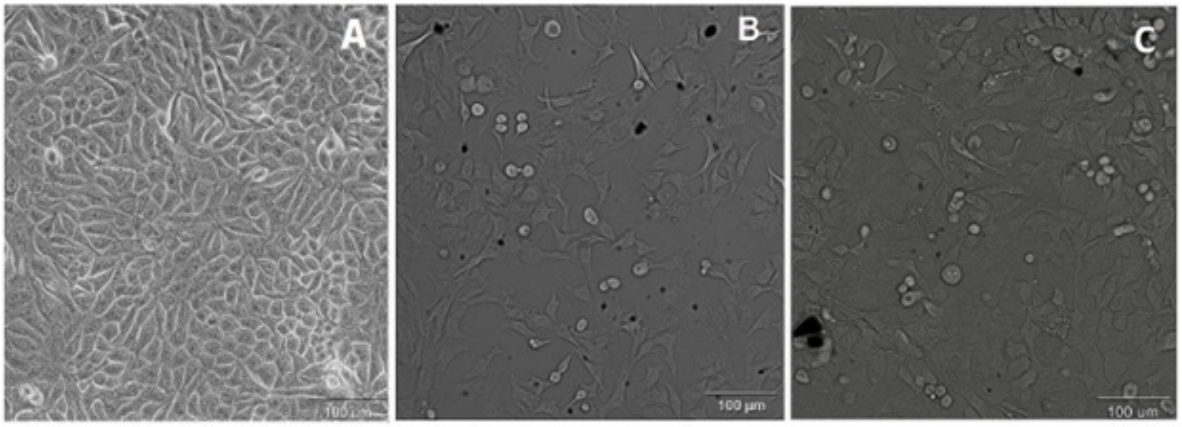

Figure 2. A549 cell line morphology. A: Unexposed cells and after 24 hours of exposure to 50 µg/ml concentration of B: Fe_2O_3, and C: Fe_3O_4 nanoparticles

statistically significant for 10 µg/ml concentration in 72 hours of exposure ($P=0.053$).

Mitochondrial Membrane Potential rate

The potential of the mitochondrial membrane at both times of exposure to all concentrations of hematite nanoparticles (except 10 µg/ml at 72 hours) was less than the control group and had a concentration-dependent trend ($P<0.05$). The effect of increasing the exposure time factor on decreasing the MMP of cells exposed to hematite nanoparticles at concentrations of 10 and 50 µg/ml was positive, while at other concentrations, it was negative (Figure 5). Mitochondrial membrane potential at 24- and 72-h exposure to magnetite nanoparticles was less than the control group and showed a concentration and time-dependent trend ($P<0.05$).

The MMP rate after 24-hour exposure of A549 cells at concentrations of 10 and 50 µg/ml of hematite and magnetite nanoparticles was lower for the magnetite, but this phenomenon was not statistically significant at 10 µg/ml concentration ($P=0.058$). The A549 cells exposed to the magnetite and hematite nanoparticles at the concentrations of 100 and 250 µg/ml, respectively, demonstrated a lower mitochondrial membrane potential for hematite nanoparticles compared to magnetite nanoparticles ($P<0.05$). The MMP produced by the exposed A549 cells at 72-hour exposure time for all concentrations of magnetite nanoparticles was lower than hematite nanoparticles, which was not significant at the 50 µg/ml concentration ($P=0.071$).

Intracellular GSH rate

The decrease in glutathione content of the A549 cell line exposed to hematite and magnetite nanoparticles had a concentration and time-dependent trend. The rate of intracellular glutathione at 24-hour exposure to all concentrations except 250 µg/ml of hematite nanoparticles and concentrations of 100 and 250 µg/ml of magnetite nanoparticles was higher than that in the control group ($P<0.05$), while at all concentrations at 72-hour exposure time was lower than that in the control group ($P<0.05$).

The results showed that the intracellular glutathione content at exposure to concentrations of ≤ 50 µg/ml at 24-hour exposure time to magnetite nanoparticles was higher than that at exposure to hematite nanoparticles ($P<0.05$) (Figure 6).

Apoptosis – Necrosis rate

The incidence of apoptosis-necrosis at exposure of the

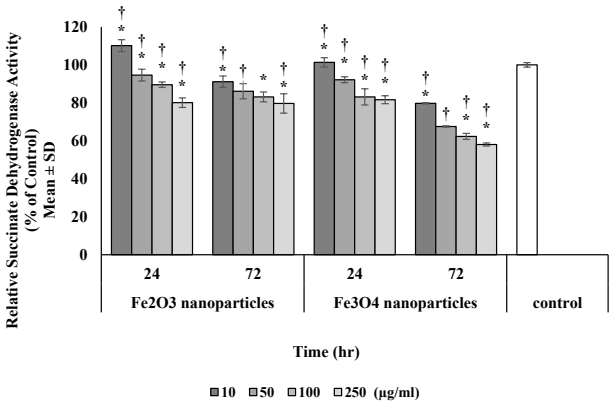

Figure 3. A549 cell line SDH activity in exposure to hematite and magnetite nanoparticles
(†=Statistically significant difference vs. Control and *=Statistically significant difference vs. Iron oxide nanoparticles (n=3, $P\leq0.05$))

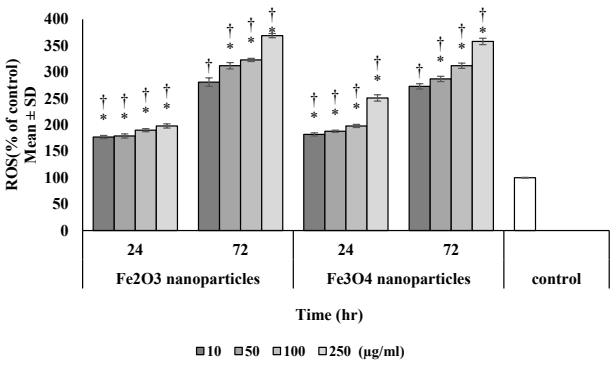

Figure 4. ROS generation in A549 cells exposed to hematite and magnetite nanoparticles
(†=Statistically significant difference vs. Control and *=Statistically significant difference vs. Iron oxide nanoparticles (n=3, $P\leq0.05$))

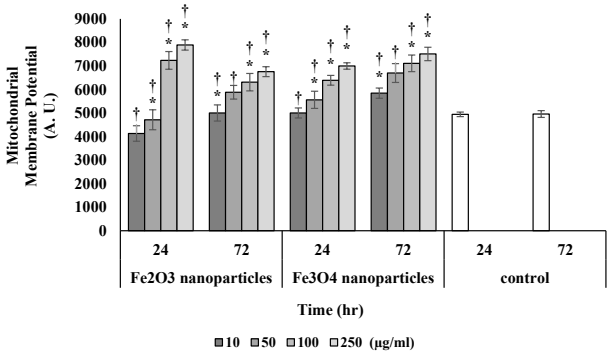

Figure 5. Reduction of mitochondrial membrane potential of the A549 cell line in exposure to hematite and magnetite nanoparticles
(†=Statistically significant difference vs. Control and *=Statistically significant difference vs. Iron oxide nanoparticles (n=3, $P\leq0.05$))

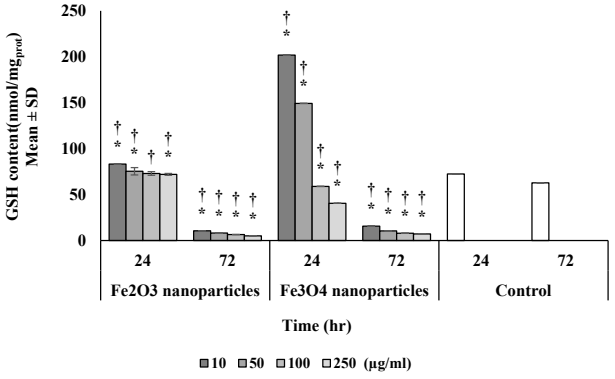

Figure 6. Intracellular glutathione content in exposure to hematite and magnetite nanoparticles
(†=Statistically significant difference vs. Control and *=Statistically significant difference vs. Iron oxide nanoparticles (n=3, $P\leq0.05$))

A549 cell line with different concentrations of hematite and magnetite nanoparticles showed a concentration and time-dependent trend, and was higher than the control group ($P<0.05$). The apoptosis-necrosis rates at exposure to all concentrations of magnetite nanoparticles in all exposure times were lower than those at exposure to hematite nanoparticles ($P<0.05$) (Figure 7).

Discussion

Iron oxide nanoparticles are among the most widely used nanoparticles in medical and industrial processes (36-38), due to their physicochemical properties and industrial capability to manufacture them in different sizes and shapes, as well as their availability (39,40). The production and consumption of iron oxide nanoparticles could lead to respiratory exposure and an increased rate of biomarkers of oxidative stress in exposed groups (41).

This study showed that human lung A549 cell lines exposed to hematite and magnetite iron oxide nanoparticles had an increased cell mortality rate and morphological change. Some authors also reported impaired cell membrane function followed by increased exposure time to iron oxide nanoparticles, demonstrating altered cytoskeletal integrity and cell morphology (42). The incidence of toxicity and cell death of the A549 cell lines in the present study also demonstrated that concentration and exposure were time-dependent, which could be explained by a higher probability of nanoparticle penetration into the cells and lysosome destruction (43). Iron is usually known as a cellular micronutrient at low concentrations, but with increasing iron concentration, it could be concentration-dependent cytotoxic (44).

The increase in A549 cell death observed in this study could be attributed to the participation of iron oxide nanoparticles in intensifying the Fenton reaction, resulting in a higher ROS generation rate compared to the unexposed cells, which has been identified by researchers as the cause of peroxidation and cell death (42,45). An increase in the rate of intracellular glutathione content in the presence of iron oxide nanoparticles in this study

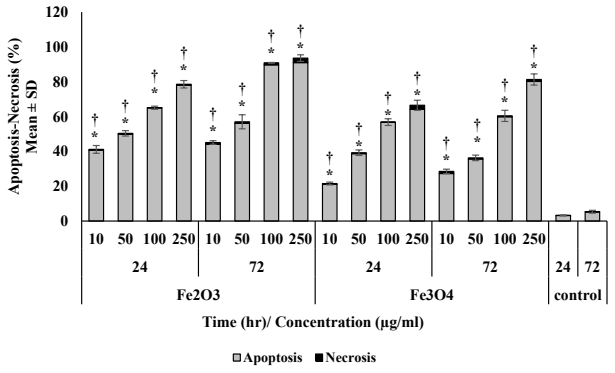

Figure 7. Apoptosis-Necrosis rate in A549 cell line exposed to hematite and magnetite nanoparticles
(†=Statistically significant difference vs. Control and *=Statistically significant difference vs. Iron oxide nanoparticles (n=3, $P\leq0.05$))

can be considered as an antioxidant defense mechanism against ROS generation (46), which modulates the rate of cell death (47,48). This stress activates antioxidant defense mechanisms, including the Nrf2 pathway, which enhances the synthesis of glutathione as a protective response to counteract oxidative stress (49). Hence, the decrease in cell death rate obtained from the apoptosis-necrosis test at exposure to magnetite nanoparticles compared to hematite nanoparticles can be due to the increase in intracellular glutathione, followed by an increase in oxidative stress. Schieber and Chandel reported the role of a slight increase in intracellular ROS in increasing glutathione content and cellular activity (47), which may lead to stimulating the activity of enzymes involved in glutathione regeneration, such as mitochondrial SDH activity. In the study of Watanabe et al, the exposure of A549 cell lines to magnetite nanoparticles was observed to increase apoptosis; at the same time, the effect on the activity of SDH was lower than apoptosis (50), which confirms the results of the present study. Another author reported that Lysosomes increase the rate of oxidative attacks and the vulnerability of other internal cell organs such as mitochondria and nuclei by producing activated ions from iron nanoparticles, and possibly, increase the incidence of A549 cell lines apoptosis, similar to the results of the present study (51).

In this study, the cell mortality rate of the human lung A549 cell lines exposed to hematite nano-cylinders was higher than that of magnetite nano-spheres. Nanoparticle morphology is one of the factors facilitating the intracellular absorption of nanoparticles (52). The results of studies show that the intracellular adsorption of rod and disk particles is much higher compared to spherical particles. Some other studies have also reported that nano-cylinder iron oxide has more toxic effects than its spherical shape, which could be due to the effect of nanoparticle appearance on the resulting magnetic field, an increase in surface-to-volume ratio, and more damage to cell membranes (40,53). Few authors have demonstrated that the permeability of cylinder nanoparticles was higher than spherical nanoparticles into the cell (54,55). Non-spherical nanoparticles having sharp edges could cause instability in lysosomal membranes and increase inflammatory toxicity. Lee et al reported that rod hematite nanoparticles accumulate in the cytoplasm, while the spherical shapes of iron oxides were stored in vacuoles, and this phenomenon may cause rod hematite nanoparticles to have more necrotic properties than iron oxide nano-spheres in cellular macrophages (40). However, in other studies, the permeability of rod nanoparticles has been reported to be lower than spherical nanoparticles, which showed a direct relationship with the increase in the length of rod nanoparticles (56,57). Accumulation of protein around nanoparticles is another deterministic factor in reducing the rate of cytotoxicity (42). In some studies,

protein accumulation around spherical nanoparticles was reported to be more than rod nanoparticles (58,59); at the same time, contradictory results were also stated by other researchers (60). Therefore, the existence of contradictory information about the effect of nanoparticle shape on cytotoxicity indicates the need for further studies (61).

The chemical structure of nanoparticles could be a factor in cell viability (40,62). Hematite iron oxide nanoparticles are converted to trivalent Fe^{+3} cations inside the cell, while magnetite nanoparticles produce both Fe^{+2} and Fe^{+3} cations. The greater tendency of hematite nanoparticles to participate in the Fenton reaction could be a result of their chemical structure and production of trivalent iron compound (27), and justifies higher toxicity and cell death rates in comparison to magnetite nanoparticles. However, divalent iron oxide nanoparticles, such as magnetite, have a high affinity for participating in the Fenton reaction cycle and production of hydroxyl ions (44,63), but ferritin is a protein that prevents toxicity by reducing the concentration of divalent ions. Ferritin, on the other hand, is a frequent intracellular protein with the capability of lowering oxidative stress by converting Fe^{+2} to Fe^{+3}, catalyzed by the ferroxidase enzyme, and stored inside the ferritin protein. Ferritin stores divalent iron ions within its nucleus and reduces the production of free radicals (64,65). Also, recent studies have highlighted the crucial role of ferritin in regulating iron homeostasis and mitigating oxidative stress by converting Fe^{2+} to Fe^{3+} and storing it within its core. This process not only reduces the production of free radicals but also protects cells from iron-induced toxicity (66). The affinity of ferritin protein for oxidizing Fe^{+2} to Fe^{+3} could justify the reduced toxicity of magnetite compared to hematite nanoparticles in the present study. To further validate our hypothesis, future studies should consider implementing a Ferritin Binding Assay to examine the direct interaction between ferritin and Fe^{2+} ions in the presence of magnetite nanoparticles. This experiment could provide valuable insights into the mechanism by which ferritin mitigates iron-induced toxicity and offer further evidence to support its role in reducing magnetite toxicity. We recommend that such experiments be considered in future investigations to strengthen our findings.

Iron oxide nanoparticles with different shapes and chemical structures have been used in recent years. Though the chemical structure, as well as the shape of nanoparticles, could have some bearing on the safe use of nanoparticles, this study examined the cytotoxicity of the two widely used iron oxide nanoparticles (hematite nano-cylinder and magnetite nano-sphere from US Research Nanomaterials, Inc. products). These results showed that hematite nanoparticles were more toxic than magnetite nanoparticles in the human lung A549 cell line. Considering the findings of this study on iron oxide nanoparticles and the limited available scientific information, further studies are recommended.

Conclusion

In this study, we compared the toxicity of hematite nano-cylinders and magnetite nano-sphere iron oxide nanoparticles on the human lung A549 cell line. Our findings indicate that both types of nanoparticles exhibit concentration and exposure time-dependent cytotoxicity, but hematite nanoparticles demonstrated a higher toxicity level than magnetite nanoparticles. The increased cell mortality and morphological changes observed in A549 cells exposed to hematite are likely due to the greater propensity of these nanoparticles to participate in the Fenton reaction, generating higher levels of reactive oxygen species (ROS) and leading to increased oxidative stress. Moreover, the hematite's nano-cylinder shape might enhance cellular absorption and cause more significant disruption of cellular structures when compared to magnetite's spherical shape. The results underscore the importance of considering both structural and chemical properties of iron oxide nanoparticles when evaluating their potential health impacts. Specifically, hematite's ability to produce trivalent iron (Fe^{3+}) compounds and its higher oxidative stress induction highlight the need for careful regulation and further investigation into its use in industrial and medical applications. Conversely, the relatively lower toxicity of magnetite, which can convert between Fe^{2+} and Fe^{3+} and is better managed by cellular antioxidant mechanisms like ferritin, suggests it may be a safer alternative under similar exposure conditions. Given the widespread use of iron oxide nanoparticles, our study emphasizes the critical need for ongoing toxicological research to better understand their health effects and to guide the development of safer nanoparticle formulations. Future research should focus on a broader range of nanoparticle shapes, sizes, and compositions, as well as in vivo studies, to fully elucidate the mechanisms of toxicity and to inform safer practices in the production and application of these nanomaterials.

Acknowledgements

The authors gratefully acknowledge the financial and administrative support provided by the Research Deputy of Shahid Beheshti University of Medical Sciences. We also extend our sincere thanks to the Air Pollution Research Center of Iran University of Medical Sciences for their valuable collaboration.

Authors' contributions

Conceptualization: Athena Rafieepour, Mansour Rezazadeh Azari.
Data curation: Athena Rafieepour.
Formal Analysis: Athena Rafieepour.
Funding acquisition: Mansour Rezazadeh Azari.
Investigation: Athena Rafieepour, Rasoul Nasiri.

Methodology: Athena Rafieepour.
Project administration: Mansour Rezazadeh Azari.
Resources: Mansour Rezazadeh Azari.
Software: Athena Rafieepour.
Supervision: Mansour Rezazadeh Azari, Jalalpour Ahmad Jaktaji.
Validation: Mansour Rezazadeh Azari, Jalalpour Ahmad Jaktaji.
Visualization: Athena Rafieepour.
Writing – original draft: Athena Rafieepour.
Writing – review & editing: Rasoul Nasiri, Jalalpour Ahmad Jaktaji.

Competing interests

The authors declare no competing interests.

Ethics issues

This study was approved by Shahid Beheshti University of Medical Sciences (Ethical code: IR.SBMU.PHNS.REC.1396.38).

Funding

The authors of this study are grateful to the Shahid Beheshti University of Medical Sciences for providing laboratory facilities and financial support for the present study (Grant No. IR.SBMU.PHNS.REC.1396.38).

References

1. Nasiri R, Motesaddi Zarandi S, Bayat M, Amini A. Design a protocol to investigate the effects of climate change in vivo. Environ Res. 2022;212(Pt D):113482. doi: 10.1016/j.envres.2022.113482.
2. Rasoulzadeh H, Sheikhmohammadi A, Alinejad N, Alipour MR, Hadei M, Aghaei Zarch SM, et al. Investigation of behaviours of diclofenac adsorption onto different adsorbents of carbon-aerogel by the kinetic and isotherm non-linear models. Int J Environ Anal Chem. 2024;104(18):7103-22. doi: 10.1080/03067319.2022.2162390.
3. Krismanuel H, Hairunisa N. The effects of air pollution on respiratory problems: a literature review. Poltekita J Ilmu Kesehat. 2024;18(1):1-15. doi: 10.33860/jik.v18i1.3151.
4. Aksu Demirezen D, Yıldız Y, Yılmaz Ş, Demirezen Yılmaz D. Green synthesis and characterization of iron oxide nanoparticles using *Ficus carica* (common fig) dried fruit extract. J Biosci Bioeng. 2019;127(2):241-5. doi: 10.1016/j.jbiosc.2018.07.024.
5. Rahman MM, Khan SB, Jamal A, Faisal M, Aisiri AM. Iron oxide nanoparticles. In: Rahman MM, ed. Nanomaterials. London, UK: IntechOpen; 2011. doi: 10.5772/27698.
6. Arias LS, Pessan JP, Vieira AP, de Lima TM, Delbem AC, Monteiro DR. Iron oxide nanoparticles for biomedical applications: a perspective on synthesis, drugs, antimicrobial activity, and toxicity. Antibiotics (Basel). 2018;7(2):46. doi: 10.3390/antibiotics7020046.
7. Czaplik W, Kischkewitz J, Spiegelhauer S. Red Iron-Oxide Pigments with Improved Colour Values. Google Patents; 2020.
8. Porter AL, Youtie J. How interdisciplinary is nanotechnology? J Nanopart Res. 2009;11(5):1023-41. doi: 10.1007/s11051-009-9607-0.
9. Lu K. Nanoparticulate Materials: Synthesis, Characterization, and Processing. New Jersey: John Wiley & Sons; 2012.
10. Roberts SM, James RC, Williams PL. Principles of Toxicology: Environmental and Industrial Applications. 4th ed. John Wiley & Sons; 2022.
11. Dadfar SM, Roemhild K, Drude NI, von Stillfried S, Knüchel R, Kiessling F, et al. Iron oxide nanoparticles: diagnostic, therapeutic and theranostic applications. Adv Drug Deliv Rev. 2019;138:302-25. doi: 10.1016/j.addr.2019.01.005.
12. Inshakova E, Inshakov O. World market for nanomaterials: structure and trends. MATEC Web Conf. 2017;129:02013. doi: 10.1051/matecconf/201712902013.
13. Shukla S, Jadaun A, Arora V, Sinha RK, Biyani N, Jain VK. In vitro toxicity assessment of chitosan oligosaccharide coated iron oxide nanoparticles. Toxicol Rep. 2015;2:27-39. doi: 10.1016/j.toxrep.2014.11.002.
14. Organisation for Economic Co-operation and Development (OECD). List of Manufactured Nanomaterials and List of Endpoints for Phase One of the Sponsorship Programme for the Testing of Manufactured Nanomaterials: Revision. Paris: OECD; 2010. p. 1-16.
15. Cortajarena AL, Ortega D, Ocampo SM, Gonzalez-García A, Couleaud P, Miranda R, et al. Engineering iron oxide nanoparticles for clinical settings. Nanobiomedicine (Rij). 2014;1:2. doi: 10.5772/58841.
16. Kashanian F, Habibi-Rezaei M, Bagherpour AR, Seyedarabi A, Moosavi-Movahedi AA. Magnetic nanoparticles as double-edged swords: concentration-dependent ordering or disordering effects on lysozyme. RSC Adv. 2017;7(86):54813-22. doi: 10.1039/c7ra08903a.
17. Fischer HC, Chan WC. Nanotoxicity: the growing need for in vivo study. Curr Opin Biotechnol. 2007;18(6):565-71. doi: 10.1016/j.copbio.2007.11.008.
18. Nel A, Xia T, Mädler L, Li N. Toxic potential of materials at the nanolevel. Science. 2006;311(5761):622-7. doi: 10.1126/science.1114397.
19. Oberdörster G, Oberdörster E, Oberdörster J. Nanotoxicology: an emerging discipline evolving from studies of ultrafine particles. Environ Health Perspect. 2005;113(7):823-39. doi: 10.1289/ehp.7339.
20. Service RF. Health and safety research slated for sizable gains. Science. 2007;315(5814):926. doi: 10.1126/science.315.5814.926a.
21. Donaldson K, Stone V, Tran CL, Kreyling W, Borm PJ. Nanotoxicology. Occup Environ Med. 2004;61(9):727. doi: 10.1136/oem.2004.013243.
22. Praphawatvet T, Peters JI, Williams RO. Inhaled nanoparticles–an updated review. Int J Pharm. 2020;587:119671. doi: 10.1016/j.ijpharm.2020.119671.
23. Patil US, Adireddy S, Jaiswal A, Mandava S, Lee BR, Chrisey DB. In vitro/in vivo toxicity evaluation and quantification of iron oxide nanoparticles. Int J Mol Sci. 2015;16(10):24417-50. doi: 10.3390/ijms161024417 .
24. Anjali, Jha SK, Kuanr BK. Synthesis and characterization of iron oxide nanoparticles (IONPs) and their cytotoxicity effects on lung epithelial carcinoma cells. AIP Conf Proc. 2017;1832(1):050110. doi: 10.1063/1.4980343.
25. Yadav M, Niveria K, Sen T, Roy I, Verma AK. Targeting nonapoptotic pathways with functionalized nanoparticles for cancer therapy: current and future perspectives. Nanomedicine (Lond). 2021;16(12):1049-65. doi: 10.2217/nnm-2020-0443.

26. Sengul AB, Asmatulu E. Toxicity of metal and metal oxide nanoparticles: a review. Environ Chem Lett. 2020;18(5):1659-83. doi: 10.1007/s10311-020-01033-6.
27. Singh N, Jenkins GJ, Asadi R, Doak SH. Potential toxicity of superparamagnetic iron oxide nanoparticles (SPION). Nano Rev. 2010;1. doi: 10.3402/nano.v1i0.5358.
28. Akter M, Sikder MT, Rahman MM, Ullah A, Hossain KFB, Banik S, et al. A systematic review on silver nanoparticles-induced cytotoxicity: physicochemical properties and perspectives. J Adv Res. 2018;9:1-16. doi: 10.1016/j.jare.2017.10.008.
29. Rafieepour A, Rezazadeh Azari M, Peirovi H, Khodagholi F, Pourahmad Jaktaji J, Mehrabi Y, et al. Investigation of the effect of magnetite iron oxide particles size on cytotoxicity in A549 cell line. Toxicol Ind Health. 2019;35(11-12):703-13. doi: 10.1177/0748233719888077.
30. Gangwal S, Brown JS, Wang A, Houck KA, Dix DJ, Kavlock RJ, et al. Informing selection of nanomaterial concentrations for ToxCast in vitro testing based on occupational exposure potential. Environ Health Perspect. 2011;119(11):1539-46. doi: 10.1289/ehp.1103750.
31. Selvamani V. Stability studies on nanomaterials used in drugs. In: Mohapatra SS, Ranjan S, Dasgupta N, Mishra RK, Thomas S, eds. Characterization and Biology of Nanomaterials for Drug Delivery. Elsevier; 2019. p. 425-44. doi: 10.1016/b978-0-12-814031-4.00015-5.
32. Jahanbani J, Ghotbi M, Shahsavari F, Seydi E, Rahimi S, Pourahmad J. Selective anticancer activity of superparamagnetic iron oxide nanoparticles (SPIONs) against oral tongue cancer using in vitro methods: the key role of oxidative stress on cancerous mitochondria. J Biochem Mol Toxicol. 2020;34(10):e22557. doi: 10.1002/jbt.22557.
33. Dey A, Manna S, Chattopadhyay S, Mondal D, Chattopadhyay D, Raj A, et al. *Azadirachta indica* leaves mediated green synthesized copper oxide nanoparticles induce apoptosis through activation of TNF-α and caspases signaling pathway against cancer cells. J Saudi Chem Soc. 2019;23(2):222-38. doi: 10.1016/j.jscs.2018.06.011.
34. Wypij M, Jędrzejewski T, Ostrowski M, Trzcińska J, Rai M, Golińska P. Biogenic silver nanoparticles: assessment of their cytotoxicity, genotoxicity and study of capping proteins. Molecules. 2020;25(13):3022. doi: 10.3390/molecules25133022.
35. Kaplan A, Kutlu HM, Ciftci GA. Fe3O4 nanopowders: genomic and apoptotic evaluations on A549 lung adenocarcinoma cell line. Nutr Cancer. 2020;72(4):708-21. doi: 10.1080/01635581.2019.1643031.
36. Ali A, Zafar H, Zia M, Ul Haq I, Phull AR, Ali JS, et al. Synthesis, characterization, applications, and challenges of iron oxide nanoparticles. Nanotechnol Sci Appl. 2016;9:49-67. doi: 10.2147/nsa.S99986.
37. Pellico J, Llop J, Fernández-Barahona I, Bhavesh R, Ruiz-Cabello J, Herranz F. Iron oxide nanoradiomaterials: combining nanoscale properties with radioisotopes for enhanced molecular imaging. Contrast Media Mol Imaging. 2017;2017:1549580. doi: 10.1155/2017/1549580.
38. Liu ZM, Wu SH, Jia SY, Qin FX, Zhou SM, Ren HT, et al. Novel hematite nanorods and magnetite nanoparticles prepared from MIL-100(Fe) template for the removal of As(V). Mater Lett. 2014;132:8-10. doi: 10.1016/j.matlet.2014.06.059.
39. Laurent S, Saei AA, Behzadi S, Panahifar A, Mahmoudi M. Superparamagnetic iron oxide nanoparticles for delivery of therapeutic agents: opportunities and challenges. Expert Opin Drug Deliv. 2014;11(9):1449-70. doi: 10.1517/17425247.2014.924501.
40. Lee JH, Ju JE, Kim BI, Pak PJ, Choi EK, Lee HS, et al. Rod-shaped iron oxide nanoparticles are more toxic than sphere-shaped nanoparticles to murine macrophage cells. Environ Toxicol Chem. 2014;33(12):2759-66. doi: 10.1002/etc.2735.
41. Pelclova D, Zdimal V, Kacer P, Fenclova Z, Vlckova S, Syslova K, et al. Oxidative stress markers are elevated in exhaled breath condensate of workers exposed to nanoparticles during iron oxide pigment production. J Breath Res. 2016;10(1):016004. doi: 10.1088/1752-7155/10/1/016004.
42. Buyukhatipoglu K, Clyne AM. Superparamagnetic iron oxide nanoparticles change endothelial cell morphology and mechanics via reactive oxygen species formation. Journal of biomedical materials research Part A. 2011;96(1):186-95. doi: 10.1002/jbm.a.32972.
43. Lee SY, Kim IY, Heo MB, Moon JH, Son JG, Lee TG. Global proteomics to study silica nanoparticle-induced cytotoxicity and its mechanisms in HepG2 cells. Biomolecules. 2021;11(3):375. doi: 10.3390/biom11030375.
44. Tvrdá E, Lukáč N, Lukáčová J, Jambor T, Massányi P. Dose- and time-dependent in vitro effects of divalent and trivalent iron on the activity of bovine spermatozoa. Biol Trace Elem Res. 2015;167(1):36-47. doi: 10.1007/s12011-015-0288-5.
45. Pourcelot E, Lénon M, Mobilia N, Cahn JY, Arnaud J, Fanchon E, et al. Iron for proliferation of cell lines and hematopoietic progenitors: Nailing down the intracellular functional iron concentration. Biochim Biophys Acta. 2015;1853(7):1596-605. doi: 10.1016/j.bbamcr.2015.03.009.
46. Núñez MT, Gallardo V, Muñoz P, Tapia V, Esparza A, Salazar J, et al. Progressive iron accumulation induces a biphasic change in the glutathione content of neuroblastoma cells. Free Radic Biol Med. 2004;37(7):953-60. doi: 10.1016/j.freeradbiomed.2004.06.005.
47. Schieber M, Chandel NS. ROS function in redox signaling and oxidative stress. Curr Biol. 2014;24(10):R453-62. doi: 10.1016/j.cub.2014.03.034.
48. Armstrong JS, Steinauer KK, Hornung B, Irish JM, Lecane P, Birrell GW, et al. Role of glutathione depletion and reactive oxygen species generation in apoptotic signaling in a human B lymphoma cell line. Cell Death Differ. 2002;9(3):252-63. doi: 10.1038/sj.cdd.4400959.
49. Ngo V, Duennwald ML. Nrf2 and oxidative stress: a general overview of mechanisms and implications in human disease. Antioxidants (Basel). 2022;11(12):2345. doi: 10.3390/antiox11122345.
50. Watanabe M, Yoneda M, Morohashi A, Hori Y, Okamoto D, Sato A, et al. Effects of Fe3O4 magnetic nanoparticles on A549 cells. Int J Mol Sci. 2013;14(8):15546-60. doi: 10.3390/ijms140815546.
51. Bardestani A, Ebrahimpour S, Esmaeili A, Esmaeili A. Quercetin attenuates neurotoxicity induced by iron oxide nanoparticles. J Nanobiotechnology. 2021;19(1):327. doi: 10.1186/s12951-021-01059-0.
52. Zhu X, Vo C, Taylor M, Smith BR. Non-spherical micro- and nanoparticles in nanomedicine. Mater Horiz. 2019;6(6):1094-121. doi: 10.1039/c8mh01527a.
53. Sun Z, Worden M, Wroczynskyj Y, Manna PK, Thliveris JA, van Lierop J, et al. Differential internalization of brick shaped iron oxide nanoparticles by endothelial cells. J Mater Chem B. 2016;4(35):5913-20. doi: 10.1039/c6tb01480a.

54. Shao D, Lu MM, Zhao YW, Zhang F, Tan YF, Zheng X, et al. The shape effect of magnetic mesoporous silica nanoparticles on endocytosis, biocompatibility and biodistribution. Acta Biomater. 2017;49:531-40. doi: 10.1016/j.actbio.2016.11.007.
55. Ma N, Wu FG, Zhang X, Jiang YW, Jia HR, Wang HY, et al. Shape-dependent radiosensitization effect of gold nanostructures in cancer radiotherapy: comparison of gold nanoparticles, nanospikes, and nanorods. ACS Appl Mater Interfaces. 2017;9(15):13037-48. doi: 10.1021/acsami.7b01112.
56. Qiu Y, Liu Y, Wang L, Xu L, Bai R, Ji Y, et al. Surface chemistry and aspect ratio mediated cellular uptake of Au nanorods. Biomaterials. 2010;31(30):7606-19. doi: 10.1016/j.biomaterials.2010.06.051.
57. Chithrani BD, Chan WC. Elucidating the mechanism of cellular uptake and removal of protein-coated gold nanoparticles of different sizes and shapes. Nano Lett. 2007;7(6):1542-50. doi: 10.1021/nl070363y.
58. García-Álvarez R, Hadjidemetriou M, Sánchez-Iglesias A, Liz-Marzán LM, Kostarelos K. In vivo formation of protein corona on gold nanoparticles. The effect of their size and shape. Nanoscale. 2018;10(3):1256-64. doi: 10.1039/c7nr08322j.
59. Deng ZJ, Mortimer G, Schiller T, Musumeci A, Martin D, Minchin RF. Differential plasma protein binding to metal oxide nanoparticles. Nanotechnology. 2009;20(45):455101. doi: 10.1088/0957-4484/20/45/455101.
60. Madathiparambil Visalakshan R, González García LE, Benzigar MR, Ghazaryan A, Simon J, Mierczynska-Vasilev A, et al. The influence of nanoparticle shape on protein corona formation. Small. 2020;16(25):e2000285. doi: 10.1002/smll.202000285.
61. Behzadi S, Serpooshan V, Tao W, Hamaly MA, Alkawareek MY, Dreaden EC, et al. Cellular uptake of nanoparticles: journey inside the cell. Chem Soc Rev. 2017;46(14):4218-44. doi: 10.1039/c6cs00636a.
62. Klein S, Sommer A, Distel LV, Neuhuber W, Kryschi C. Superparamagnetic iron oxide nanoparticles as radiosensitizer via enhanced reactive oxygen species formation. Biochem Biophys Res Commun. 2012;425(2):393-7. doi: 10.1016/j.bbrc.2012.07.108.
63. Sharp P. The molecular basis of copper and iron interactions. Proc Nutr Soc. 2004;63(4):563-9. doi: 10.1079/pns2004386.
64. Pease C, Rücker T, Birk T. Review of the evidence from epidemiology, toxicology, and lung bioavailability on the carcinogenicity of inhaled iron oxide particulates. Chem Res Toxicol. 2016;29(3):237-54. doi: 10.1021/acs.chemrestox.5b00448.
65. Knovich MA, Storey JA, Coffman LG, Torti SV, Torti FM. Ferritin for the clinician. Blood Rev. 2009;23(3):95-104. doi: 10.1016/j.blre.2008.08.001.
66. Mesquita G, Silva T, Gomes AC, Oliveira PF, Alves MG, Fernandes R, et al. H-Ferritin is essential for macrophages' capacity to store or detoxify exogenously added iron. Sci Rep. 2020;10(1):3061. doi: 10.1038/s41598-020-59898-0.